

**Magnetic-field effects on nonlinear electrostatic-wave Landau damping**

F. Valentini and P. Veltri

*Università della Calabria, Dipartimento di Fisica and Istituto Nazionale di Fisica della Materia, Unità di Cosenza, I-87030 Arcavacata di Rende, Italy*

A. Mangeney

*LESIA, Observatoire de Paris, Section de Meudon 5, place Jules Janssen, 92195 Meudon Cedex, France*

(Received 28 July 2004; revised manuscript received 14 October 2004; published 4 January 2005)

A numerical code, which solves the Vlasov-Poisson system of equations for an electron magnetized plasma with motionless ions, is presented. The numerical integration of the Vlasov equation has been performed using the “splitting method” and the cylindrical geometry in the velocity space is used to describe the motion of the particles around the external field. The time evolution of an electrostatic wave, propagating perpendicularly to the background magnetic field, is numerically studied in both the linear and nonlinear regimes, for different values of the ratio  $\gamma$  between the electron oscillation time in a sinusoidal potential well and the electron cyclotron period. It is shown that the external magnetic field plays very different roles, depending on the values of the initial wave amplitude. When the initial amplitude is less than some threshold, the magnetic field prevents the Landau damping of the electrostatic wave (Bernstein-Landau paradox). When the wave amplitude is above the threshold, for intermediate values of  $\gamma$  the presence of a background magnetic field allows for the electric energy dissipation at variance with the behavior of electrostatic wave in unmagnetized plasma, while for high  $\gamma$  values once again the magnetic field prevents the damping.

DOI: 10.1103/PhysRevE.71.016402

PACS number(s): 52.35.Ra, 52.25.Dg, 52.25.Xz, 52.35.Mw

**I. INTRODUCTION**

In unmagnetized plasmas, wave particle interactions can give rise to wave damping, also when collisions are absent. In the linear Landau theory [1], the damping is produced by the interaction between the wave and the electrons with velocity  $v \approx v_\phi$ , where  $v_\phi$  is the phase velocity of the wave. The physical content of the linear interaction is conceptually quite simple: electrons whose velocity is just below the wave phase velocity in their *tail-on collision* with the wave gain some energy, while electrons whose velocity is just above lose it (*head-on collisions*). So when the former particles are more numerous than the latter the wave exhibits exponential damping.

For times longer than  $T_t = \sqrt{(m/eEk)}$ , the so-called trapping time, which represents the characteristic oscillation time of a particle in a sinusoidal potential well ( $e$  and  $m$  are, respectively, the electron charge and mass, while  $E$  is the electric field amplitude of the wave and  $k$  its wave vector), nonlinear effects start becoming effective, as first studied by O’Neil [2], who found that in such case the oscillatory-like motion of the resonant particles must be taken into account. This oscillatory motion should prevent any further damping, in that each particle has now time to make both *tail-on* and *head-on collisions* with the wave, so that the net energy exchange between wave and particle, when averaged on time, is null.

Recent numerical simulations [3–5] and experimental analyses [6] support the O’Neil view, in that when starting with a sufficiently large initial wave amplitude, in the final asymptotic state wave damping is stopped. Moreover, following the time evolution of a small but finite amplitude wave, they showed the formation of vortices in the phase

space in the resonant region of the electron distribution function. The formation of these structures represents a typical signature of the nonlinear Landau damping.

The results of numerical simulations have also been substantiated by Lancellotti and Dornig [7], who showed, by studying Landau damping as a bifurcation problem, that there exist critical initial states that mark the transition between the Landau scenario, in which the electric field is definitively damped to zero, and the O’Neil scenario, in which the Landau damping is stopped. In magnetized collisionless plasmas, on the contrary, as shown by Bernstein [8], electrostatic waves, propagating perpendicular to an external uniform magnetic field  $\mathbf{B}_0$  ( $k_\parallel=0$ ), are totally undamped. Using the Landau approach, Bernstein studied the dispersion relation of electrostatic waves in a magnetized plasma and found a peculiar behavior for the perpendicular propagation. Considering the limit of vanishing magnetic field and then putting  $k_\parallel=0$ , one recovers the well-known features of the Landau-damped oscillations, but if one considers first the perpendicular propagation and then puts  $B_0=0$ , the spectrum is not damped and it is composed of all the harmonics of the electron cyclotron frequency. The continuity between magnetized and unmagnetized case was not respected (Bernstein-Landau paradox).

The first explanation of this discontinuous behavior has been furnished by Baldwin and Rowlands [9], who developed a theory about the damping of the Bernstein waves; they showed that, when the magnetic field approaches zero, the Bernstein modes behave as usual electrostatic waves in an unmagnetized plasma, because the electron cyclotron frequency decreases with the magnetic field and the cyclotron period becomes much larger than the above defined trapping time of the resonant particles. This causes an overlap of all harmonics of  $\omega_B$  (the electron cyclotron frequency) and the

waves are damped according to the usual Landau damping rate of electrostatic modes, so the Landau's solution is a superposition of many Bernstein modes in the limit  $\omega_B \rightarrow 0$ .

In the presence of an external magnetic field  $\mathbf{B}_0$ , the Landau-like damping is visible only during a time smaller than the electron cyclotron period  $T_B = 2\pi/\omega_B$ . At each cyclotron period, the magnetic field reestablishes the phase coherence. These conclusions have been confirmed by Kamimura *et al.* [10] who used two-dimensional (2D) and  $2\frac{1}{2}$ D dipole expansion codes to simulate electrostatic waves in a magnetized plasma. The problem has been treated also by Sukhorukov and Stubbe [11], who solved numerically the dispersion relation of the Bernstein waves and showed that, in the magnetized case, the Landau damping is visible in the first gyroperiod, for very brief time transients, but the waves are not damped for very long times.

From the discussion above, it is then clear that both large amplitudes of the wave and large values of the background magnetic field are able to stop Landau damping. It is then worth studying what happens when both effects are present—i.e., what are the nonlinear effects on electrostatic wave damping in magnetized plasmas. In fact, the presence of a background magnetic field can prevent the nonlinear saturation of the Landau damping, in that electrons turning in the magnetic field have not sufficient time to perform *head-on collisions*, if the electron cyclotron period is much shorter than the trapping time. When the two times are of the same order, the particle oscillation in the electrostatic potential well and the particle circular motion in the background magnetic field can interact in a very complicated way. The parameter  $\gamma = T_t/T_B$ —i.e., the ratio between trapping time and electron cyclotron period—plays a key role in the study of non linear effects on electrostatic waves in a magnetized plasma.

For this reason, in the present work, performing kinetic numerical simulations, we discuss the time evolution of an electrostatic wave, propagating in a magnetized plasma perpendicularly to the background magnetic field, as function of its amplitude on the one hand and of the  $\gamma$  value on the other hand. We will show that, as long as these two parameters vary, different regimes are found characterized by different time behaviors.

The organization of the paper is as follows. In Sec. II the cylindrical Vlasov-Poisson code is described, with a discussion about the energy conservation test we have performed on the code. Section III is devoted to the description of the numerical results for the electric oscillations and for the evolution of the electron distribution function in the velocity space, in both unmagnetized and magnetized cases. A discussion of the numerical results is presented in Sec. IV.

## II. A CYLINDRIC VLASOV-POISSON CODE

### A. Mathematical problem

The set of equations describing electrostatic waves propagating perpendicularly with respect to a background magnetic field  $\mathbf{B}_0$ , in its simpler form, can finally be reduced to a problem which is 1D in the physical space and 2D in the velocity space:

$$\frac{\partial f}{\partial t} + V_x \frac{\partial f}{\partial x} + (E_x + V_y B_0) \frac{\partial f}{\partial V_x} - V_x B_0 \frac{\partial f}{\partial V_y} = 0, \quad (1)$$

$$\frac{\partial E_x}{\partial x} = \int f dV_x dV_y - 1. \quad (2)$$

In the above equations,  $f(x, V_x, V_y, t)$  is the electron distribution function (the ions are considered as a motionless background of neutralizing positive charge),  $\mathbf{E}(x, t)$  is the electric field, and the magnetic field  $\mathbf{B}_0$  is along the  $z$  direction (only space variations along  $x$  direction are allowed). Moreover, the time is normalized to the inverse of the electron plasma frequency  $\omega_{pe}$ , the velocity to the electron thermal velocity  $v_{th}$ , and consequently,  $E$  to  $m\omega_{pe}v_{th}/\sigma|q|$  and  $B_0$  to  $m\omega_{pe}c/\sigma|q|$  ( $\sigma$  is the sign of the charge and  $c$  is the speed of light). Finally,  $f$  is normalized to the equilibrium density  $n_0$ .

Using polar coordinates [ $v = \sqrt{V_x^2 + V_y^2}$  and  $\varphi = \arctan(V_y/V_x)$ ] in the velocity space, the set of equations (1) and (2) can be recast in the following form:

$$\frac{\partial f}{\partial t} + V_x \frac{\partial f}{\partial x} - B_0 \frac{\partial f}{\partial \varphi} + \frac{1}{v} \frac{\partial}{\partial v} [v E_v(\varphi) f] + \frac{1}{v} \frac{\partial}{\partial \varphi} [E_\varphi(\varphi) f] = 0, \quad (3)$$

$$\frac{\partial E_x}{\partial x} = \rho(x) = \int f v dv d\varphi - 1, \quad (4)$$

where  $f = f(x, v, \varphi, t)$ ,  $E_\varphi(\varphi) = -E_x \sin \varphi$  and  $E_v(\varphi) = E_x \cos \varphi$  are the electric-field components, in polar coordinates.

The initial condition represents a Maxwellian function in the velocity space, over which a modulation in the physical space with amplitude  $A$  and wave vector  $k$  is superposed:

$$f(x, v, \varphi, 0) = \frac{1}{\sqrt{2\pi}} \exp[-v^2/2] [1 + A \cos(kx)]. \quad (5)$$

### B. Numerical method

Using polar coordinates in the velocity space, to perform numerical integration, represents the main peculiarity of the code we have built up. Actually, in these coordinates, the numerical integration of the Vlasov equation in the velocity space is considerably simplified, because the rotation of the particles in the  $V_x$ - $V_y$  plane is reduced to a translation in  $\varphi$ . This allows for an extremely accurate energy conservation, as we will show in the next subsection. The Vlasov equation (3) has then been numerically solved in the phase space, using the well-known splitting scheme, in the electrostatic limit [12], coupled with a finite-difference upwind scheme. The approach is similar to what is usually called the *semi-Lagrangian* transport scheme in meteorology [13–18]. The Poisson equation is integrated in the Fourier space by using a fast Fourier transform (periodic boundary conditions in the  $x$  direction are assumed).

The simulation domain in the phase space is given by  $D = [0, L_x] \times [0, v_{max}] \times [0, 2\pi]$ , where  $L_x = 2\pi/k$  is the length of the physical simulation box and  $v_{max} = 6$ . Outside the ve-

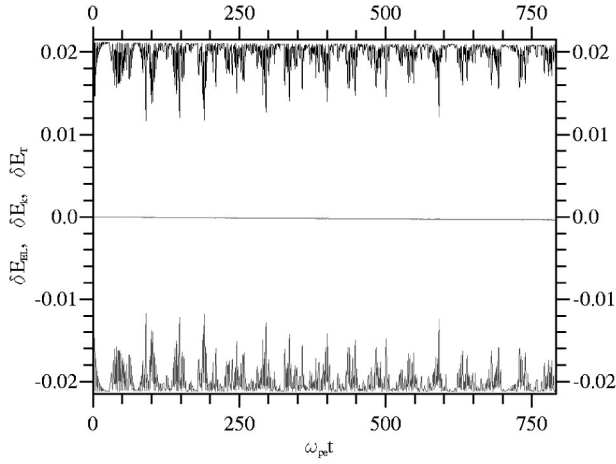


FIG. 1. Long-time evolution of the fluctuations of electric energy  $\delta E_{el}(t) = E_{el}(t) - E_{el}(0)$ , kinetic energy  $\delta E_K(t) = E_K(t) - E_K(0)$ , and total energy  $\delta E_T(t) = E_T(t) - E_T(0)$  for  $B_0 = 0.18$ ,  $A = 0.03$ , and  $k = 0.405$ .

locity simulation domain, the distribution function is put equal to zero. In the simulation domain,  $N_x$  grid points in the physical space and  $N_v \times N_\varphi$  in the velocity space have been used. Typically, a simulation is performed using  $N_x = 64$ ,  $N_v = 256$ , and  $N_\varphi = 512$  grid points. The time step  $\Delta t \approx 0.01 - 0.005$  has been chosen in order to satisfy the stability CFL (Courant-Friedrichs-Levy) condition. For advection equations in the form

$$\frac{\partial f}{\partial t} + A \frac{\partial f}{\partial x} = 0,$$

the CFL condition is  $\Delta t \leq \Delta x / |A|$ .

### C. Numerical dissipation and energy conservation

From the Vlasov equation (1), the evolution equations for the moments,

$$n = \int f d\mathbf{v}, \quad n\mathbf{V} = \int \mathbf{v} f d\mathbf{v}, \quad n\epsilon = \frac{1}{2} \int (\mathbf{v} - \mathbf{V})^2 f d\mathbf{v},$$

can be derived. In particular, using the fact that periodic boundary conditions are imposed in the physical space, the following energy conservation relation in dimensionless units can finally be obtained:

$$E_K + E_{el} = E_T = \text{const}, \quad (6)$$

where  $E_K$  and  $E_{el}$  are, respectively, the kinetic (direct and internal) and electric energies,

$$E_K = \int \left( \frac{1}{2} n \mathbf{V}^2 + n\epsilon \right) dx, \quad E_{el} = \int \frac{E^2}{2} dx.$$

The time behavior of the energy is shown in Fig. 1 for the following set of parameters:  $A = 0.03$ ,  $k = 0.405$ , and  $B_0 = 0.18$ . The evolution is followed up to  $t = 800\omega_{pe}^{-1}$ . In this figure, the fluctuations of the kinetic energy are represented at the top, those of the electric energy at the bottom, and finally those of the total energy in the middle. While the fluctuations of the kinetic and electric energy are of the order

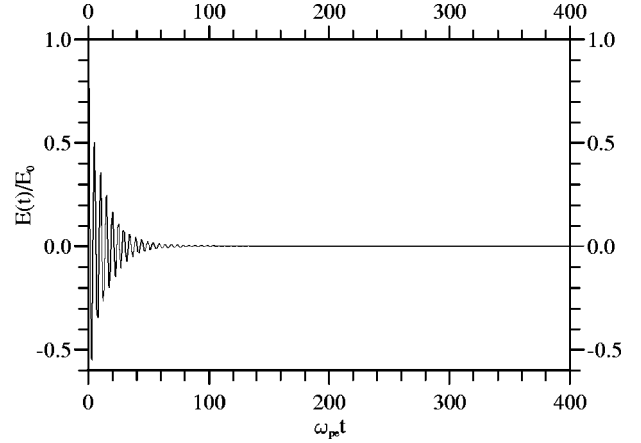


FIG. 2. Time evolution of the electric field  $E(t)/E_0$  as a function of normalized time in the unmagnetized case ( $\gamma = 0$ )  $A = 0.01$  and  $k = 0.405$ .

of  $10^{-2}$ , the total energy loss is  $|E_T(800) - E_T(0)| = 3 \times 10^{-4}$ , about two orders of magnitude smaller than kinetic and electric energy variations. The energy is then conserved all along the simulations in a very satisfactory way.

## III. NUMERICAL SIMULATIONS

As discussed in the Introduction, both numerical simulations and theoretical studies have shown that, in an unmagnetized plasma, an electrostatic wave is damped to zero if its initial perturbation amplitude is less than a critical value; otherwise, after a certain time, the damping is stopped and the wave amplitude starts oscillating around a more or less constant value. For  $k \approx 0.4$ , the critical amplitude is  $A^* \approx 0.012$  [4].

Even if our simulations have been performed in presence of a background magnetic field, we will show that is very useful to classify the wave behavior according to the value of the initial perturbation amplitude (subcritical or supercritical). Each of these two situations has, moreover, been studied in function of the increasing value of the background magnetic field, whose importance is measured by the previously defined parameter  $\gamma$ . In dimensionless units the expression of  $\gamma$  is reduced to  $\gamma = B_0 / \sqrt{A}$ .

### A. Subcritical simulations

In all subcritical runs we have used a value of the initial perturbation amplitude  $A = 0.01 < A^*$ . In Fig. 2, we show the time evolution of the electric field, when the external magnetic field is equal to zero and for a wave number value  $k = 0.405$  (the phase velocity of the wave is  $v_\phi \approx 3.2$ ). The damping of the oscillations is very strong and the electric energy is completely dissipated after  $t \approx 100\omega_{pe}^{-1}$ .

In Fig. 3, from the top to the bottom, we have represented, up to six electron cyclotron periods, the time evolution of the wave electric field for increasing values of the external magnetic field—i.e., increasing values of  $\gamma$ . The typical change [9,11] in Bernstein wave damping, when increasing the value of the background magnetic field, is clearly observed. In cor-

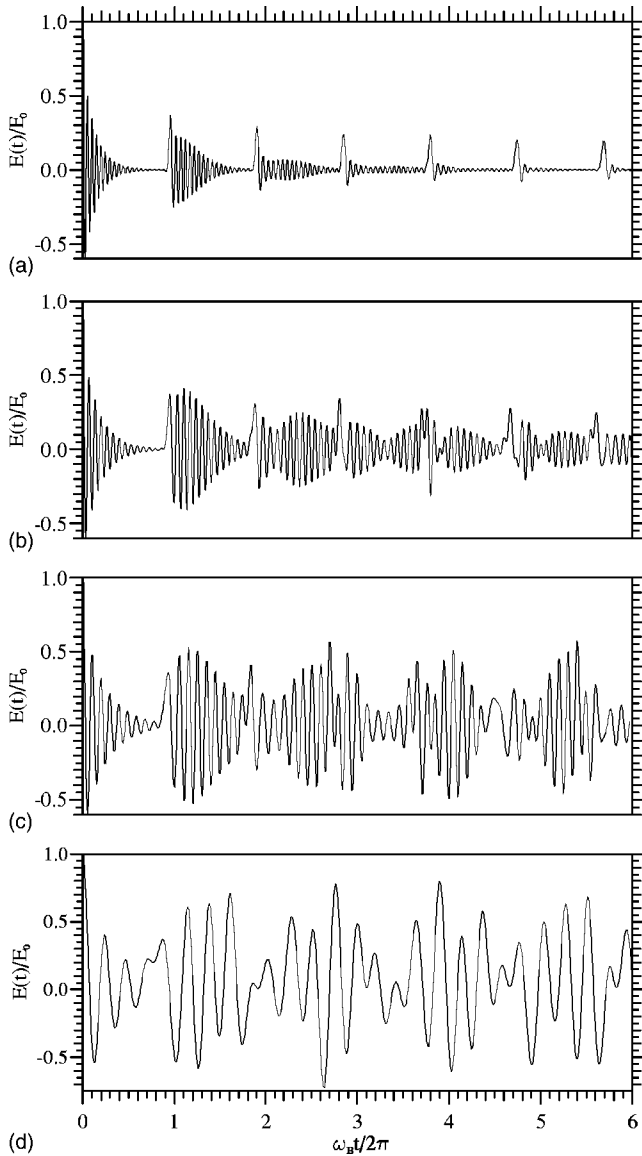


FIG. 3. Time evolution of the electric field  $E(t)/E_0$  as a function of time normalized to the electron cyclotron period for  $\gamma=0.629$  (a),  $\gamma=0.85$  (b),  $\gamma=1.25$  (c), and  $\gamma=3$  (d).  $A=0.01$  and  $k=0.405$ .

response to the multiples of the electron cyclotron periods, the magnetic field raises the amplitude of the electrostatic oscillations. When  $\gamma \approx 1$  [panel (c)]—i.e., when the electron cyclotron period is smaller than the trapping time—the electric oscillations are asymptotically no more damped; the final amplitude of the electric field is reduced only to 50% of its initial value. Finally, in panel (d), the strongly magnetized case ( $\gamma=3$ ) is shown; the effect of the Landau damping is considerably weakened, showing that the dominant effect of the magnetic field changes completely the nature of the wave-particle interaction, which is responsible for the wave damping in the unmagnetized case. Let us note that the final amplitude of undamped oscillations increases with the value of  $\gamma$ .

In correspondence to the strongest value of the magnetic field ( $\gamma=3$ ), in Fig. 4, we have reported the evolution of the electrostatic wave for three different values of the wave

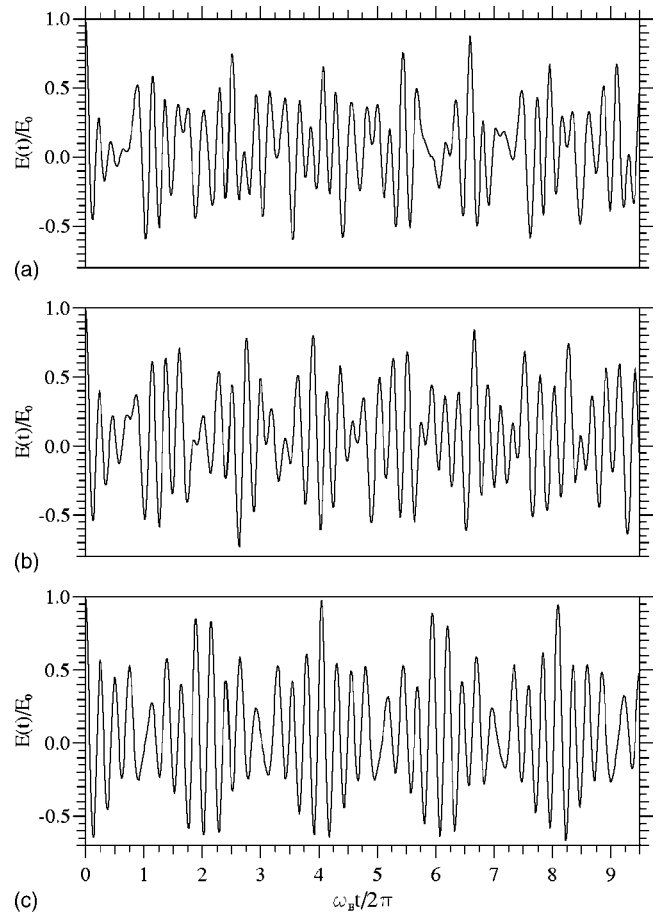


FIG. 4. Time evolution of the electric field  $E(t)/E_0$  as a function of time normalized to the electron cyclotron period for  $\gamma=3$ ,  $A=0.01$  and for three different values of the wave number,  $k \approx 0.5$  (a),  $k \approx 0.4$  (b),  $k \approx 0.3$  (c).

number ( $k=0.5, 0.4, 0.3$ ). When decreasing the value of  $k$ , the oscillations are less and less damped. Actually, as  $k$  decreases, according to the Landau's theory [1], the damping rate decreases, since the phase velocity increases and a smaller number of particles interact resonantly with the wave. For  $k=0.3$  [panel (c)], the maximum value of the wave amplitude remains almost equal to the initial wave amplitude.

### B. Supercritical simulations

In all our supercritical simulations, the initial perturbation amplitude has been chosen  $A=0.03 > A^*$ , while the wave vector is always  $k=0.405$ . In the unmagnetized case, displayed in Fig. 5(a), as expected, the effect of the Landau damping is asymptotically stopped and the electric field goes on oscillating around an approximately constant value. In panel (b), where the value of the magnetic field is very small ( $\gamma=5.77 \times 10^{-5}$ ), the behavior of the electric oscillations is rather similar to that shown in panel (a). Nevertheless, the presence of the magnetic field seems to progressively slightly reduce the amplitude of the electric-field envelope oscillations.



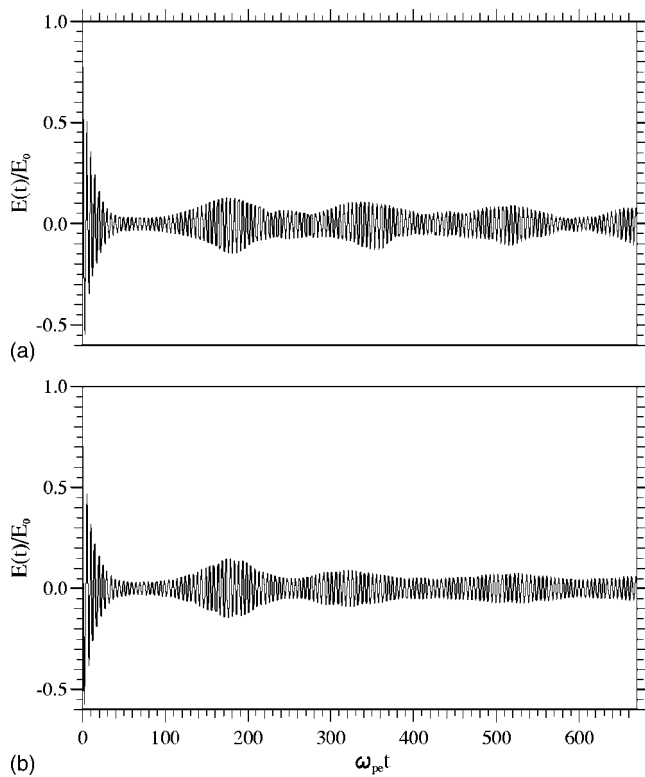


FIG. 5. Time evolution of the electric field  $E(t)/E_0$  as a function of normalized time for  $A=0.03$ ,  $k=0.405$ ,  $\gamma=0$  (a), and  $\gamma=5.77 \times 10^{-5}$  (b).

This behavior is much more evident in Fig. 6(a), where the electric-field time evolution for  $\gamma=5.77 \times 10^{-3}$  is shown. The stronger value of the external background magnetic field does not allow for the electric-field envelope oscillations. As a consequence, the wave is completely damped, even if we are in a supercritical situation, from the point of view of the wave amplitude. In this region of parameters, the role of the background magnetic field is inverted with respect to subcritical situations. The presence of a magnetic field, which prevents damping in the subcritical runs, now evidently competes with nonlinear effects and allows for a complete wave damping.

When increasing the value of the background magnetic field ( $\gamma=0.173$ ), a peculiar phenomenon occurs. As is shown in Fig. 6(b) after wave damping, isolated electrostatic wave packets, separated in time by the electron cyclotron period, appear. Increasing more and more the background magnetic field, the isolated structures increase both their duration and their amplitude and progressively collapse, forming a quasisinusoidal undamped wave structure. This behavior is displayed in Fig. 6, panel (c), for  $\gamma=1.155$ .

The above results show that, both in the case where the magnetic field is absent and in the case where it is very strong, the damping of the wave is asymptotically stopped. In the first case [Fig. 5, panel (a)] the damping is prevented by the resonant wave-particle interaction and in the second one [Fig. 6, panel (c)] by the magnetic-field effect.

Moreover, the transition between the unmagnetized and magnetized cases is characterized by the competition of the

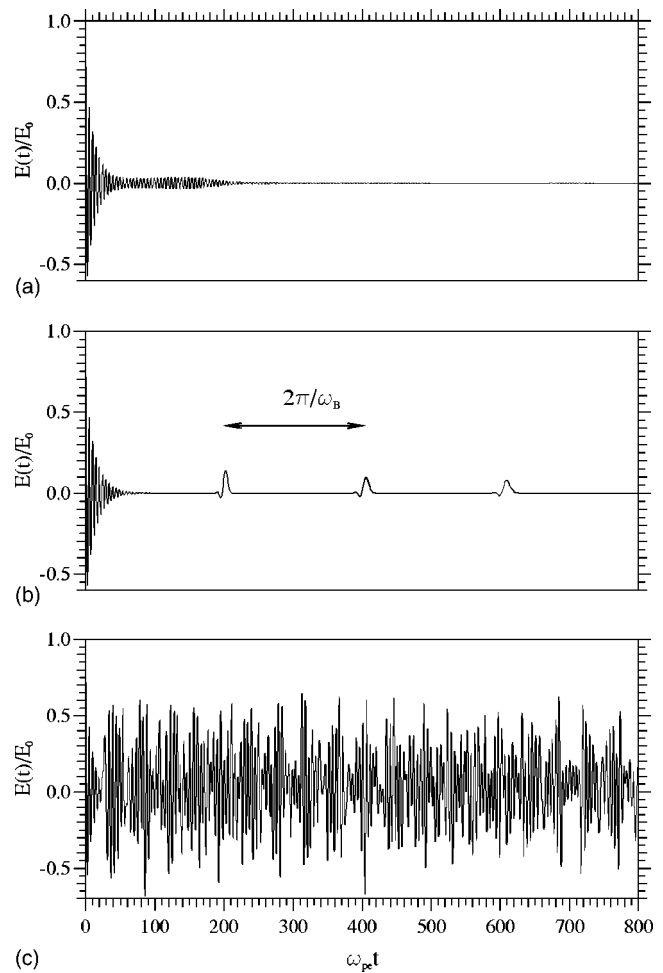


FIG. 6. Time evolution of the electric field  $E(t)/E_0$  as a function of normalized time for  $A=0.03$ ,  $k=0.405$ , and, respectively,  $\gamma=5.77 \times 10^{-3}$  (a),  $\gamma=0.173$  (b), and  $\gamma=1.155$  (c).

trapping phenomenon and the magnetic-field effect. In fact, for intermediate values of the external field, we observe first damped oscillations [Fig. 6, panel (a)], as if the trapping phenomenon and the presence of the magnetic field canceled each other, none of them being able to sustain the electric oscillations. Then, increasing the value of  $B_0$  [Fig. 6, panel (b)], isolated electrostatic pulses appear, as if these structures were the intermediate step between plasma oscillations and Bernstein waves.

The phenomenology discussed above can be also studied by looking at the behavior of the resonant region of the electron distribution function in the velocity space under the effect of the magnetic field.

Figure 7 shows the contour plot of the distribution for  $\gamma=5.77 \times 10^{-3}$  at six different times [corresponding to the electric signal displayed in Fig. 6(a)]. For  $t=100\omega_{pe}^{-1}$  [panel (a)], the result of the wave particle interaction is clearly visible on the contour lines in the region  $V_x \approx \pm v_\phi$ . As time goes on, the presence of the magnetic field gives rise to a rigid rotation of the distribution function in the  $V_x$ - $V_y$  plane, which can be seen in the same figure, in panels (b), (c), (d), (e), and (f). The effect of this rotation is to bring particles, which were interacting with the wave, outside the resonant

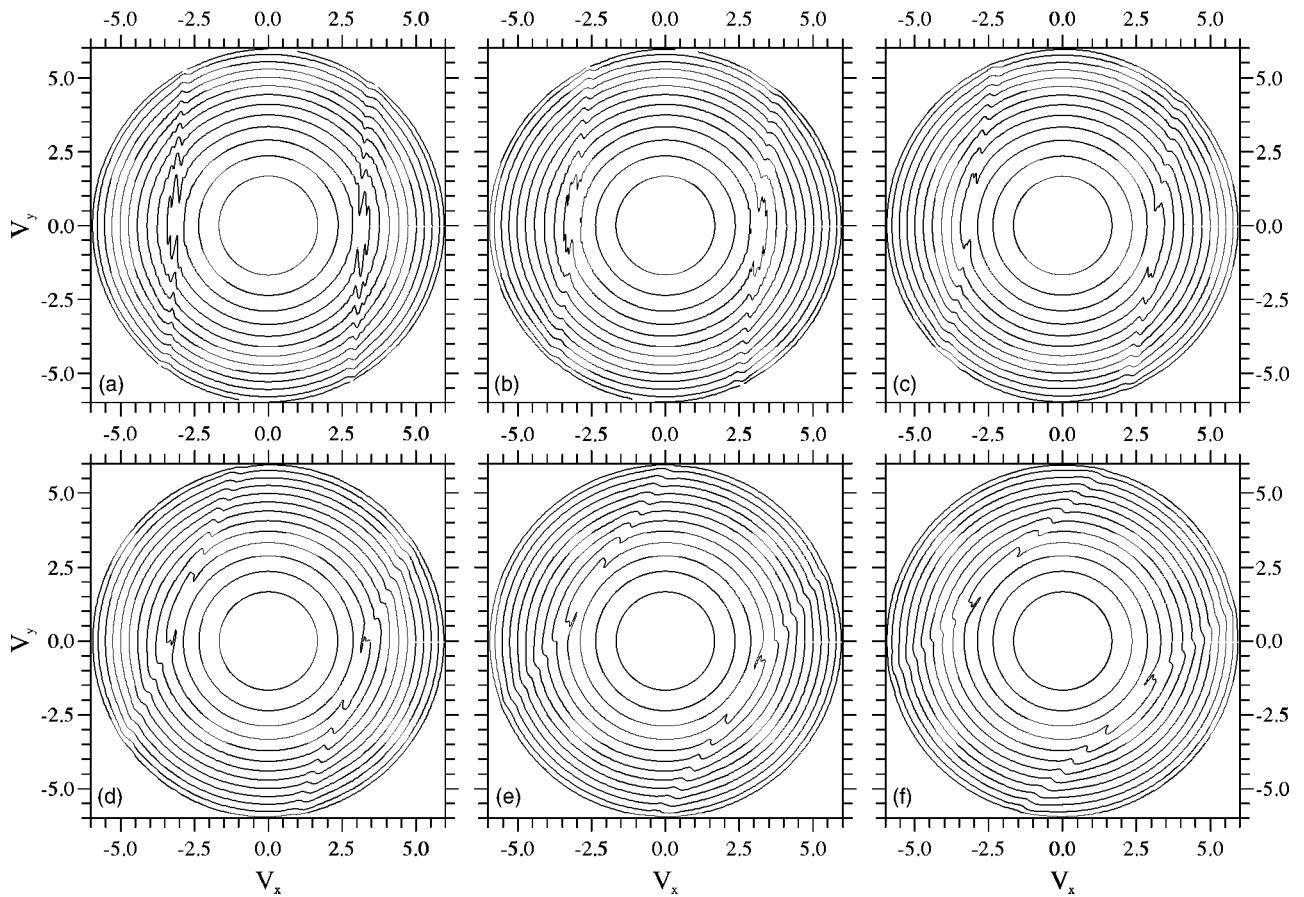


FIG. 7. Contour plot of the electron distribution function in the velocity space for  $B=0.001$  and for  $t=100\omega_{pe}^{-1}$  (a),  $t=150\omega_{pe}^{-1}$  (b),  $t=200\omega_{pe}^{-1}$  (c),  $t=400\omega_{pe}^{-1}$  (d),  $t=600\omega_{pe}^{-1}$  (e), and  $t=800\omega_{pe}^{-1}$  (f).

region, thus reducing the effect of wave trapping. In fact, the magnetic field, in half a rotation, changes the sign of  $V_x$ ; as a consequence, the kinetic energy along the  $x$  direction in the wave reference frame increases  $[(1/2)m(-V_x - v_\phi)^2 > (1/2)m(V_x - v_\phi)^2]$ , so resonant particles get enough energy to overcome the electrostatic potential barrier and to become detrapped. Obviously, each cyclotron period, particle energy decreases until trapping condition is effective and particles, which have been detrapped, once again interact resonantly with the wave [this is what happens in the case of Fig. 6(b)]. However, if the cyclotron period is very large (very weak magnetic field) the electric energy is dissipated before particles can be retrapped [Fig. 6(a)].

On the distribution function, this corresponds to a smoothing of the distortion, introduced by wave particle interaction, during the rotation. This smoothing represents the signature of the reduction of wave particle interaction, which, as a consequence, does not allow the particles to give back to the wave the energy previously gained, so no damping saturation occurs. Moreover, in this case ( $\gamma=5.77 \times 10^{-3}$ ), the magnetic field is too weak to sustain the electric oscillations, so the wave is definitively damped.

When the magnetic field is absent or very weak (for example,  $\gamma=5.77 \times 10^{-5}$ , as in Fig. 5) the rotation of the distribution function is also absent or very slow; thus, the perturbation of the distribution function contour lines, due to wave

particle interaction, is not affected by the external field (see Fig. 8, top). This means that the particles continue to exchange energy with the wave, as in the unmagnetized case, and the damping is stopped. On the other hand, for very strong magnetic fields [for example,  $B=0.18$ , as in Fig. 6(c)], the rotation is very fast and the perturbation of the distribution function disappears very quickly in the resonant region. In this case, the damping is stopped by the strong magnetic effect and no wave particle interaction is visible, as shown in Fig. 8 (bottom).

#### IV. CONCLUSIONS

The study of collective plasma effects, like Landau damping in the nonlinear regime, requires numerically solving the Vlasov equation [19]. In this paper, using a numerical code, we have studied the nonlinear regime of the wave-particle interaction in a magnetized plasma. The cylindrical geometry, used in the velocity space for the numerical integration of the Vlasov equation, is particularly effective in describing the dynamics of charged particles moving in an uniform magnetic field, because it is the natural way to describe circular motions. The cylindrical Vlasov-Poisson code has then been used to numerically investigate the propagation of electrostatic waves and the wave particle interaction in the fully nonlinear regime and in both the unmagnetized and magne-

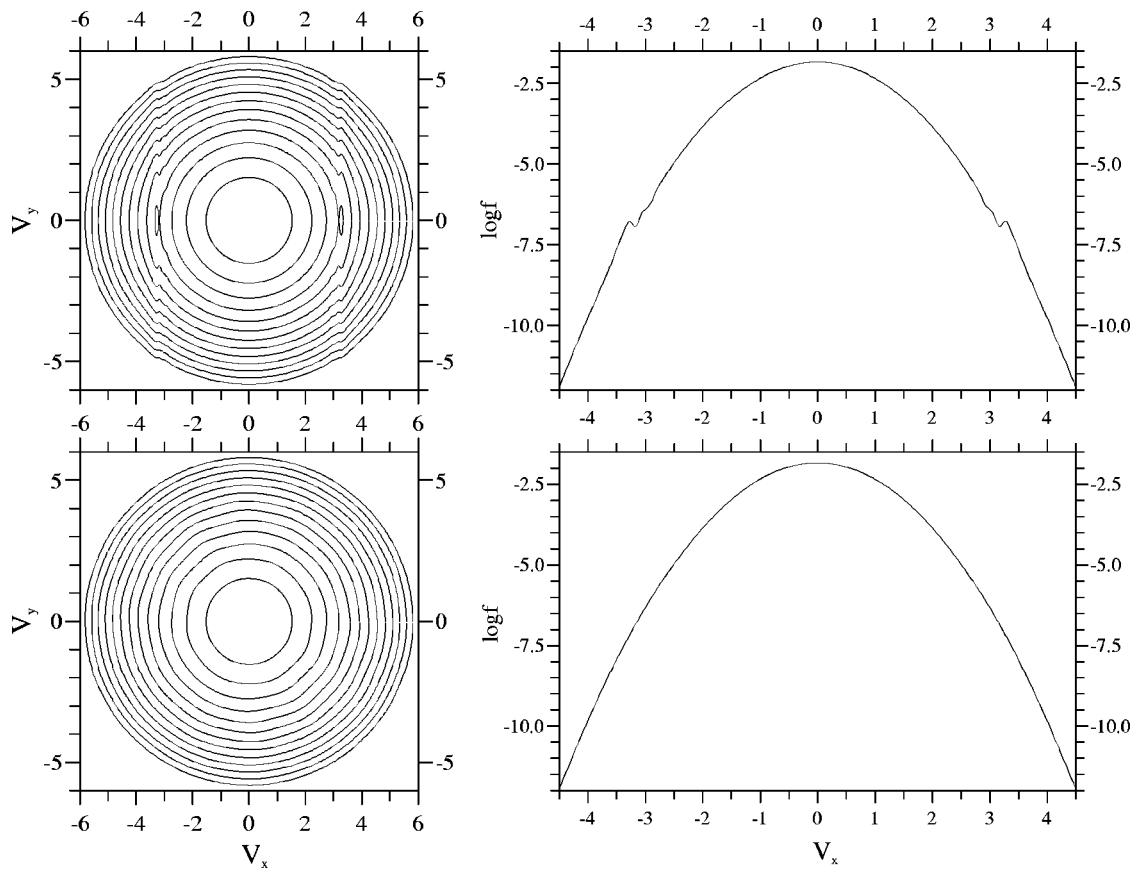


FIG. 8. Electron distribution function velocity space contour plot and its semilogarithmic plot at  $V_y=0$  as a function of  $V_x$  for  $\gamma=0$  (at the top) and  $\gamma=1.155$  (at the bottom). Both figures are represented at  $t=200\omega_{pe}^{-1}$ .

tized cases (perpendicular propagation,  $k_{\parallel}=0$ ). We have shown as the time behavior of electrostatic oscillations changes drastically as the parameter  $\gamma$  varies,  $\gamma$  being the ratio between the trapping time and electron cyclotron period. When the initial amplitude of the electrostatic perturbation is less than some threshold (subcritical situation), the effect of the background magnetic field is to sustain the electric time oscillations and to prevent the Landau damping of the wave. Our numerical results are in good agreement with results previously obtained solving linearized equations [9,11].

On the other hand, in supercritical simulations, we have found that the role of the background magnetic field totally changes, with respect to the subcritical situation. Even if in the unmagnetized case the nonlinear wave particle interaction was able to stop the wave damping, in presence of a magnetic field, we find peculiar time behaviors, as a result of the competition between nonlinear effects and the magnetic field. In both the weakly and strongly magnetized cases ( $\gamma \ll 1$  and  $\gamma > 1$ ), we observe undamped signals and the electric-field time evolution is dominated in the first case by the nonlinear effects and in the second one by the magnetic field. On the contrary, for intermediate values of  $\gamma$ , first totally damped oscillations and then isolated electrostatic pulses appear, as if these structures were the link between plasma oscillations and Bernstein modes.

Looking at the contour plot of the electron distribution function in the velocity space allowed us to give a physical interpretation to the damped oscillations, observed in supercritical runs, for intermediate values of  $\gamma$  ( $\gamma=5.77 \times 10^{-3}$ ). As we have shown, the background magnetic field produces a rigid rotation of the distribution function in the  $V_x$ - $V_y$  plane, so it brings particles, which were trapped in the wave potential well, outside the resonant region and makes the nonlinear effects no more efficient in stopping the wave damping. Moreover, the magnetic field is really too weak to sustain the oscillations by itself, as in the case  $\gamma > 1$ , and the electric energy is totally dissipated. Finally, the isolated electric pulses, which we observe increasing the value of the background field, are the result of a complicated particle dynamics, produced by the nonlinear coupling of two frequencies (trapping oscillations and circular motion in the magnetic field). The peculiarity of these structures deserves further investigation, which is, however, beyond the objectives of the present work.

#### ACKNOWLEDGMENTS

The authors wish to acknowledge F. Califano, M. Lontano, and C. Marchetto for numerous and useful discussions and suggestions.

- [1] L. D. Landau, *J. Phys. (Moscow)* **10**, 25 (1946).
- [2] T. O'Neil, *Phys. Fluids* **8**, 2255 (1965).
- [3] G. Manfredi, *Phys. Rev. Lett.* **79**, 2815 (1997).
- [4] M. Brunetti, F. Califano, and F. Pegoraro, *Phys. Rev. E* **62**, 4109 (2000).
- [5] F. Valentini, V. Carbone, P. Veltri, and A. Mangeney, *Phys. Rev. E* (to be published).
- [6] J. R. Danielson, F. Anderegg, and C. F. Driscoll, *Phys. Rev. Lett.* **92**, 245003 (2004).
- [7] C. Lancellotti and J. J. Dornig, *Phys. Rev. Lett.* **81**, 5137 (1998).
- [8] I. B. Bernstein, *Phys. Rev.* **109**, 10 (1957).
- [9] D. E. Baldwin and G. Rowlands, *Phys. Fluids* **9**, 2444 (1966).
- [10] T. Kamimura, T. Wagner, and J. M. Dawson, *Phys. Fluids* **21**, 1151 (1978).
- [11] A. I. Sukhorukov and P. Stubbe, *Phys. Plasmas* **4**, 2497 (1997).
- [12] C. Z. Cheng and Georg Knorr, *J. Comput. Phys.* **22**, 330 (1976).
- [13] A. Harten, *J. Comput. Phys.* **135**, 260 (1982).
- [14] A. Harten, *J. Comput. Phys.* **131**, 3 (1986).
- [15] A. Harten, *J. Comput. Phys.* **131**, 247 (1986).
- [16] Randall J. Leveque, *SIAM (Soc. Ind. Appl. Math.) J. Numer. Anal.* **33**, 627 (1996).
- [17] B. Van Leer, *J. Comput. Phys.* **23**, 263 (1976).
- [18] A. Mangeney, F. Califano, C. Cavazzoni, and P. Travnicek, *J. Comput. Phys.* **179**, 495 (2002).
- [19] F. Califano and M. Lontano, *Phys. Rev. E* **67**, 056401 (2003).